Applied Catalysis B: Environmental 208 (2017) 75–81

Contents lists available at ScienceDirect

Applied Catalysis B: Environmental

journal homepage: www.elsevier.com/locate/apcatb

Readily attainable spongy foam photocatalyst for promising practical photocatalysis

Shuobo Wang[a], Yihe Zhang[a,*], Tierui zhang[b], Fan Dong[c], Hongwei Huang[a,*]

[a] Beijing Key Laboratory of Materials Utilization of Nonmetallic Minerals and Solid Wastes, National Laboratory of Mineral Materials, School of Materials Science and Technology, China University of Geosciences, Beijing, 100083, China
[b] Key Laboratory of Photochemical Conversion and Optoelectronic Materials, Technical Institute of Physics and Chemistry, Chinese Academy of Sciences, Beijing, 100190, China
[c] College of Environmental & Biological Engineering, Chongqing Technology & Business University, Chongqing, 400067, China

ARTICLE INFO

Article history:
Received 27 November 2016
Received in revised form 2 February 2017
Accepted 9 February 2017
Available online 13 February 2017

Keywords:
Polyurethane foam
BiOX
Photocatalysis
Pollutants
Recycle

ABSTRACT

Photocatalysis currently remains a series of key challenges, such as difficult recovery of powder, low efficiency, etc, which grievously impede the practical application of powdery photocatalysts in environmental remediation and renewable energy generation. In this work, we integrate a flexible and porous organic matrix polyurethane foam (PUF) with nanosheet-array-like bismuth oxyhalides (BiOX) as efficient and stable photocatalysts via a facile dipping-hydrolysis means. The BiOX/PUF foam photocatalysts uncover profoundly promoted photocatalytic performance for treating multiform organic contaminants ranging from azo dye, phenol to antibiotic, in comparison with the powdery counterparts. These foam photocatalysts also display enhanced photocatalytic activity toward water splitting into H_2 evolution. Significantly, they show absorbing performance in many aspects, including high stability, easy recovery, good recycling and excellent controllability and adaptability, strongly boding for their promising practical prospect. The study may not only advance a series of practical photocatalysts for environmental control and renewable energy generation, but also have the potential to be extended to development of other high-performance photocatalytic materials.

1. Introduction

Semiconductor photocatalysts have attracted great attention owing to their unique abilities for environmental purification and energy generation [1,2]. Among the various semiconductor materials, titanium dioxide (TiO_2) has been widely researched photocatalyst because of its low cost, long-term stability, and non-toxicity.

Semiconductor photocatalysts have emerged as the most potential materials for environmental remediation and renewable energy generation in the past decades [1–6]. Advances towards an efficient photocatalyst suitable for wastewater/gaseous effluents treatment or water splitting under visible light mainly include metal oxides, oxysalt, sulfides and organic metal complexes [7–16]. In the current researches, the vast majority of photocatalysts are used as powder in the photocatalytic reaction process. It suffers from the some fatal drawbacks, such as difficult separation, weak durability, low efficiency, etc. which rigorously restrict its applications in practical photocatalysis. Thus, an enormous challenge posed for practical photocatalysis currently is how to immobilize these nanoscaled powders on certain solid substrates for easy separation and recycling for long-term effectiveness and durability [17–19]. Some pioneering work have attempted to conquer these issues, including immobilization of nanostructured photocatalysts on carbonized fiber [20], disc [21], stainless steel monoliths [22], and so on. Though some successes are achieved, they are still subjected to the low surface area and activity, complex synthesis procedure, and complicated operation [23]. Therefore, developing an easily-handled, eco-friendly and scalable protocol for preparing robust photocatalysts that simultaneously achieve high-efficiency and convenient separation/recycling is imperative and of cardinal significance.

Bismuth oxyhalides, namely BiOX (X = Cl, Br, I), have recently triggered considerable interests in the photocatalytic field due to the interesting structure-dependent photocatalytic performance that arises from their unique layered structure interleaved with $[Bi_2O_2]$ slabs and double halogen atoms slabs [24–27]. The dispersive valance band (VB) and conduction band (CB) induced by sp hybridization give rise to high mobility of the photoinduced charge

* Corresponding authors.
E-mail addresses: zyh@cugb.edu.cn (Y. Zhang), hhw@cugb.edu.cn (H. Huang).

http://dx.doi.org/10.1016/j.apcatb.2017.02.033
0926-3373/

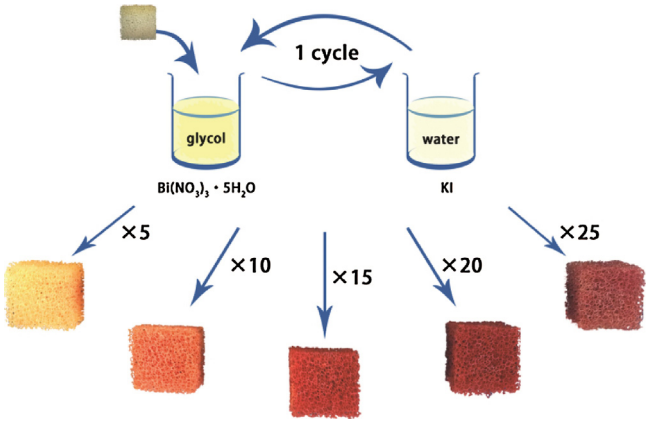

Scheme 1. Schematic illustration for PUF based-BiOI foam photocatalysts obtained by a facile dipping-hydrolysis method.

carriers [28,29]. In addition, the internal electric field resulting from the asymmetric charge distribution between $[Bi_2O_2]^{2+}$ and the halogen layers facilitates the effective separation of the photoinduced charge carriers [30,31]. Benefiting from these advantages, BiOX displays attractive photocatalytic performance, especially for photo-oxidation degradation of organic contaminants. Given the serious drawbacks of powdery photocatalyst in practical application, it would be a great step toward to develop a facile strategy to efficaciously immobilize the powdery BiOX photocatalyst on a suitable support that could simultaneously realize the efficient photocatalysis and long-term effectiveness and durability.

Herein, a three-dimensional (3D) porous and flexible organic matrix, polyurethane foam (PUF), has been introduced into this work and first reported serving as a photocatalyst support. PUF was here selected as the substrate owing to its peculiar properties, including open skeleton, high surface area and low density [32–34]. PUF fulfills all the requirements for a good support and especially, its light weight makes it capable of floating on the upper surface of an aqueous reaction system, which allows it to absorb more solar irradiations. In this work, we give a clear workable picture of an easily-handled, eco-friendly and scalable strategy for fabricating PUF based-BiOX (X = Cl, Br, I) composite photocatalysts. The BiOX nanosheets are uniformly assembled on the surface of PUF to form an interesting nanosheet-array structure. To fully assess the performance of BiOX/PUF composites, multiform contaminants ranging from azo dye, phenol to antibiotic are utilized as target, and water splitting into H_2 evolution is also monitored. The BiOX/PUF composites exhibit highly enhanced photocatalytic performance compared to the powdery counterparts. Significantly, in addition to easy recycling, BiOX/PUF is flexible and density-controllable, which allow it adaptable to reactor of all shapes and different reaction conditions. The crafty coupling between the organic matrix and BiOX photocatalyst may provide a tangible guideline to develop controllable, high-performance and practical composite photocatalyst.

2. Experimental section

2.1. Preparation of the photocatalyst

All starting materials were of analytical grade and used as received. A facile dipping-hydrolysis method was used to prepare PUF based-BiOX composite photocatalysts. 0.2 mol $Bi(NO_3)_3{\cdot}5H_2O$ was dissolved in 100 mL ethylene glycol to form solution A, and 0.2 mol KX (X = Cl, Br, I) was dissolved in 100 mL distilled water to form solution B. The PUF foams were dipped into solution A about 10 s with vigorously string and then, the PUF foams were dipped into solution B about 10 s. After that, the PUF foams were dipped back into solution A and these steps were called as one cycle. With increasing the cycle times, BiOX (X = Cl, Br, I) tend to grow on the PUF surface continuously. Then the resulting BiOX/PUF(X = Cl, Br, I) was washed repeatedly with ethanol and distilled water, and then dried at room temperature. Besides, the $BiOCl_{0.5}Br_{0.5}$/PUF, $BiOBr_{0.5}I_{0.5}$/PUF and $BiOCl_{0.5}I_{0.5}$/PUF were also synthesized using the same method.

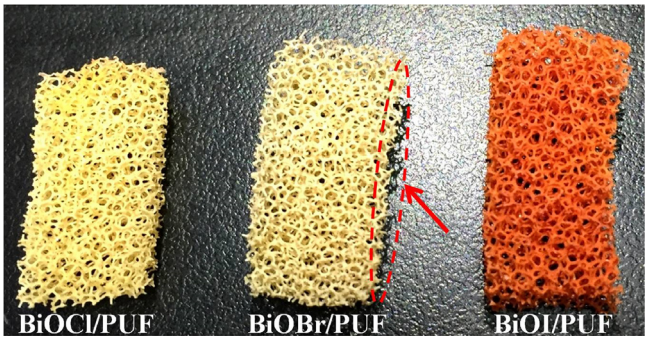

Fig. 1. Digital picture of 3D porous BiOX/PUF.

2.2. Characterization

X-ray powder diffraction (XRD) was recorded on a Bruker D8 focus with graphite monochromatized Cu Kα radiation (40 kV/40 mA). UV–vis diffuse reflectance spectra (DRS) were performed at a Varian Cary 5000 UV–vis spectrophotometer. The morphologies of the photocatalysts were analyzed by fieldemission scanning electron microscopy (SEM) on a Hitachi S-4800 instrument operated at 10.0 kV. Transmission electron microscopy (TEM) and high-resolution TEM (HRTEM) were evaluated by A JEM-2100 electron microscopy (JEOL, Japan). All the above-mentioned measurements were taken at room temperature.

2.3. Photodegradation evaluation

The photocatalytic activities of BiOX/PUF(X = Cl, Br, I) were tested by photocatalytic decomposition of methyl orange (MO), phenol and chlortetracycline under simulated solar light with a 500 W Xe lamp. In a typical procedure, the BiOX/PUF foams were put into 50 mL of MO (2×10^{-5} mol/L), phenol (10 mg/L) or chlortetracycline (50 mg/L) aqueous solution, respectively. Before photoreaction, the BiOX/PUF and reagent were magnetically stirred in darkness for 1 h to obtain an adsorption-desorption equilibrium. Later, about 3 mL of the liquid was taken at certain period time, and separated through centrifugation to obtain the supernatant. The concentration of reagent liquid was analyzed by measuring the absorbance at the characterwastic band on a Cary 5000 UV–v was spectrophotometer. The photocatalytic activities $BiOCl_{0.5}Br_{0.5}$/PUF, $BiOBr_{0.5}I_{0.5}$/PUF and $BiOCl_{0.5}I_{0.5}$/PUF were also tested by the same method.

2.4. Photocatalytic H_2 evolution

Photocatalytic H_2 production experiments were performed in photoreactor (Pyrex glass) at room temperature connected to a closed-cycle gas circulation system. A 300 W Xe lamp was used as light source. In a typical photocatalytic experiment, the cube of BiOX/PUF was put in 40 mL of distilled water with the loading of 1 wt% Pt cocatalyst, which was conducted by directly dissolving H_2PtCl_6 into the above suspension. Then, the suspension solution was stirred and irradiated (UV-light) for 30 min and entered into photoreactor with 50 mL distilled water and 10 mL methanol. The products were analyzed by gas chromatography (Labsolar-III(AG),

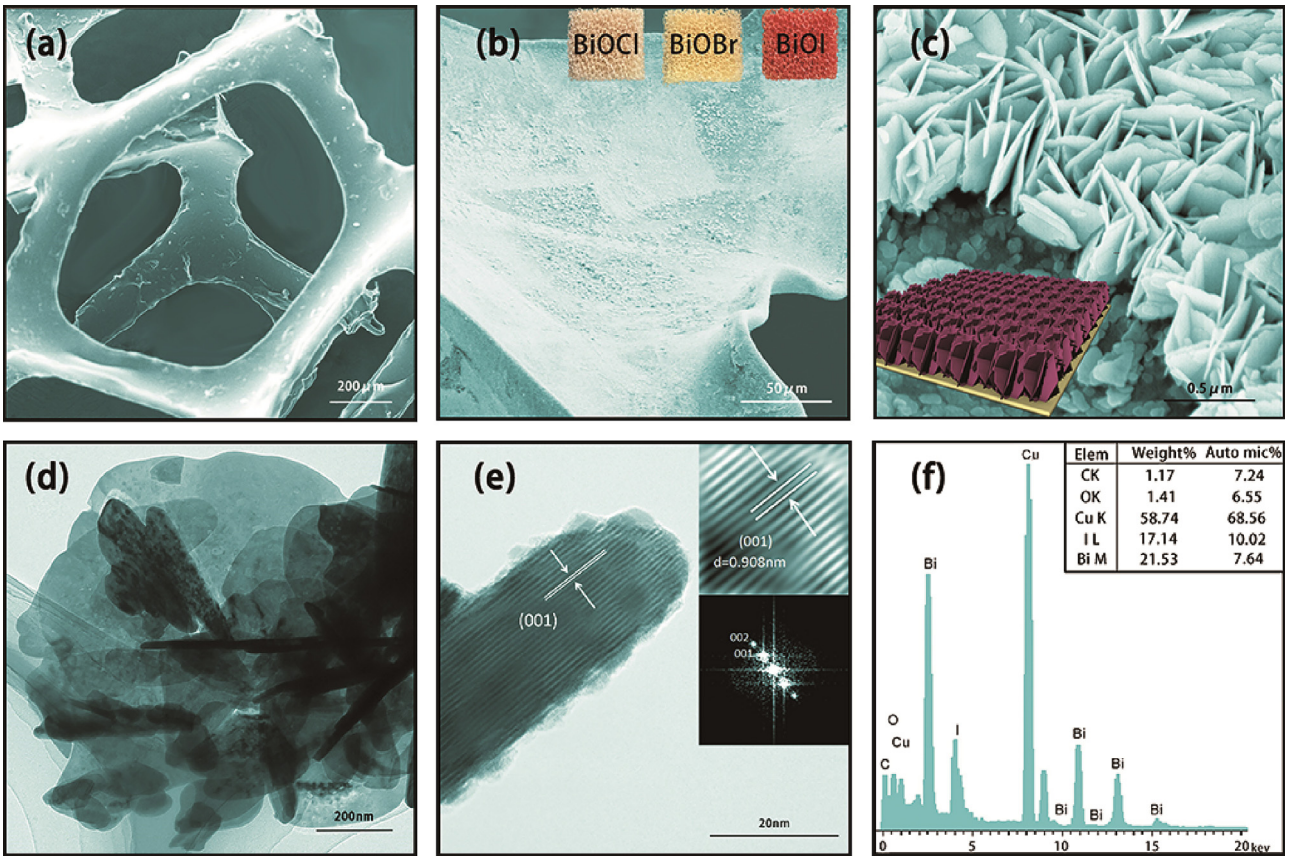

Fig. 2. (a) SEM image of PUF; (b) SEM image of BiOI/PUF foam and photographs of PUF based-BiOCl/BiOBr/BiOI foams (insets); (c) Magnified SEM image of BiOI/PUF; (d-f) TEM, HRTEM and EDX images of BiOI powder (peeled from BiOI/PUF foam).

high-purity nitrogen as a carrier gas) using a thermal conductivity detector.

2.5. Active species trapping experiment

To detect the active species generated in the photocatalytic process, methanol was chosen as a hole (h^+) scavenger, ethylene glycol (IPA) was used as a hydroxyl radical ($^\bullet OH$) scavenger [35], and nitrotetrazolium blue chloride (NBT) was employed as a superoxide radical ($^\bullet O_2^-$) scavenger [36]. Typically, BiOX/PUF with different scavengers (1 mmol) was dispersed in an aqueous solution of methyl orange (MO) (50 mL, 1×10^{-5} mol/L), and the following processes were similar to the photodegradation experiment.

3. Results and discussion

As an excellent 3D porous substrate, PUF substrate is of high stability, which cannot be degraded by BiOI (Fig. S1a). Also, there is a strong electric attraction between BiOI powder and PUF (Fig. S1b), which is beneficial to BiOX loading on the surface of PUF matrix and photocatalytic reaction. Accordingly, PUF based-BiOX composite photocatalysts are prepared via a facile dipping-hydrolysis method using PUF as a 3D porous substrate, and the different BiOX loading amount can be easily achieved by controlling the dipping cycle times (Scheme 1). Taking BiOI/PUF as a representative, BiOI have continuously grown on the PUF surface with increasing the dipping times due to that $Bi(NO_3)_3$ grasped on PUF tends to constantly react with KI to generate more BiOI (Fig. S2 and 3). Apparently, the different loading amount of BiOI could be observed directly (color from yellow to brick-red).

Fig. 1 shows the digital picture of BiOX/PUF foams. It is obvisous that the photon could easily enter and through the BiOX/PUF foam photocatalysts. SEM reveals that PUF possesses well-defined 3D macroporous networks which can serve as an excellent substrate (Fig. 2a). It shows a neat surface with the skeleton keel of 200 μm in width. As BiOX was introduced onto PUF, different BiOX/PUF foams are obtained (inset of Fig. 2b), and the BiOX powders are evenly distributed on the surface of PUF (Fig. 2b and S4). Fig. 2c shows that the loaded BiOI on PUF presents a unique nanosheet-array-like morphology, which is believed to promote the adsorption ability of reactants. Generally, the array-like structure tends to show stronger adsorption and degradation capabilities than regular powder [33]. TEM indicates that these nanosheets are very thin with an thickness of about 20 nm (Fig. 2d). HRTEM and FFT images (Fig. 2e) revealed that the exposed facet of BiOI anosheets is (001) plane, which is the active facet of BiOI favoring for charge separation. EDX further confirms the BiOI phase (Fig. 2f).

In addition to BiOX (X = Cl, Br, I) single-phase materials, the $BiOCl_{0.5}Br_{0.5}$, $BiOBr_{0.5}I_{0.5}$ and $BiOCl_{0.5}I_{0.5}$ solid-solutions are also synthesized using the same method, which has been confirmed by XRD (Fig. 3a). Construction of these solid-solutions results in adjustable absorption edge offset consecutively from 350 nm to about 700 nm (Fig. 3b), thus enabling the BiOX materials tunable band gap and photo-reduction or oxidation capabilities. As compared to a single BiOX phase, the solid-solutions with various band energy potentials may meet the diverse needs for contaminant degradation (Fig. S5), as different pollutants have their respective redox potentials.

In order to reveal the performance of PUF based-BiOX foam photocatalysts, several kinds of environmental pollutions have been employed as target. To compare the photocatalytic acivity of pow-

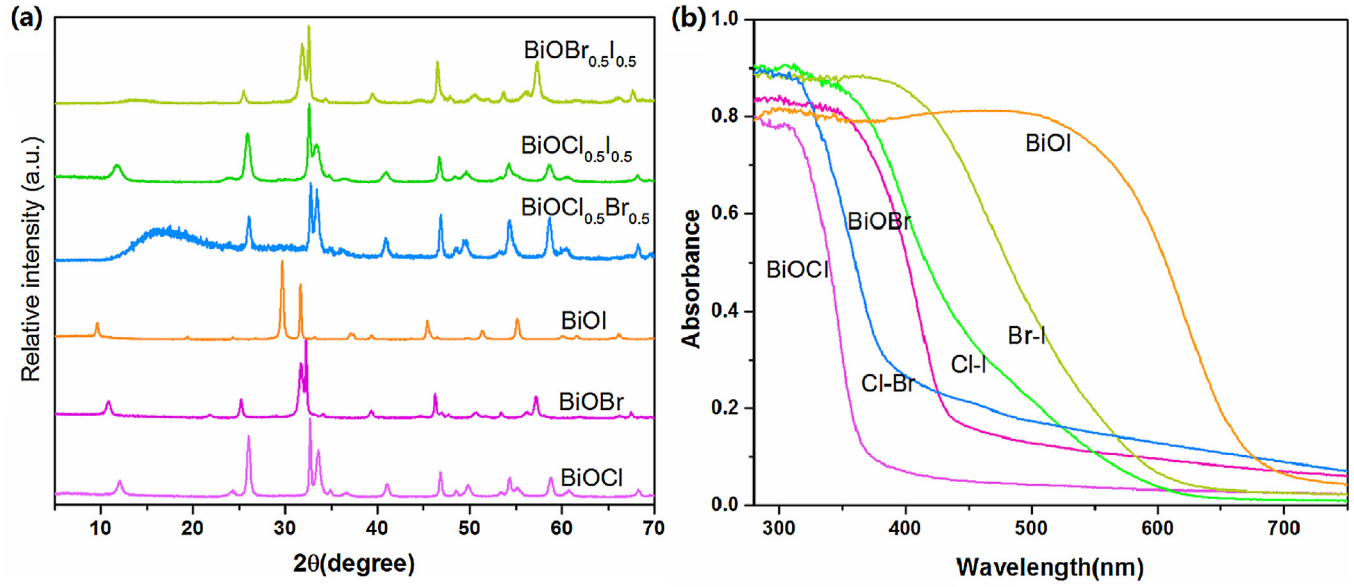

Fig. 3. (a) XRD patterns and (b) UV–vis diffuse reflectance spectra of the samples.

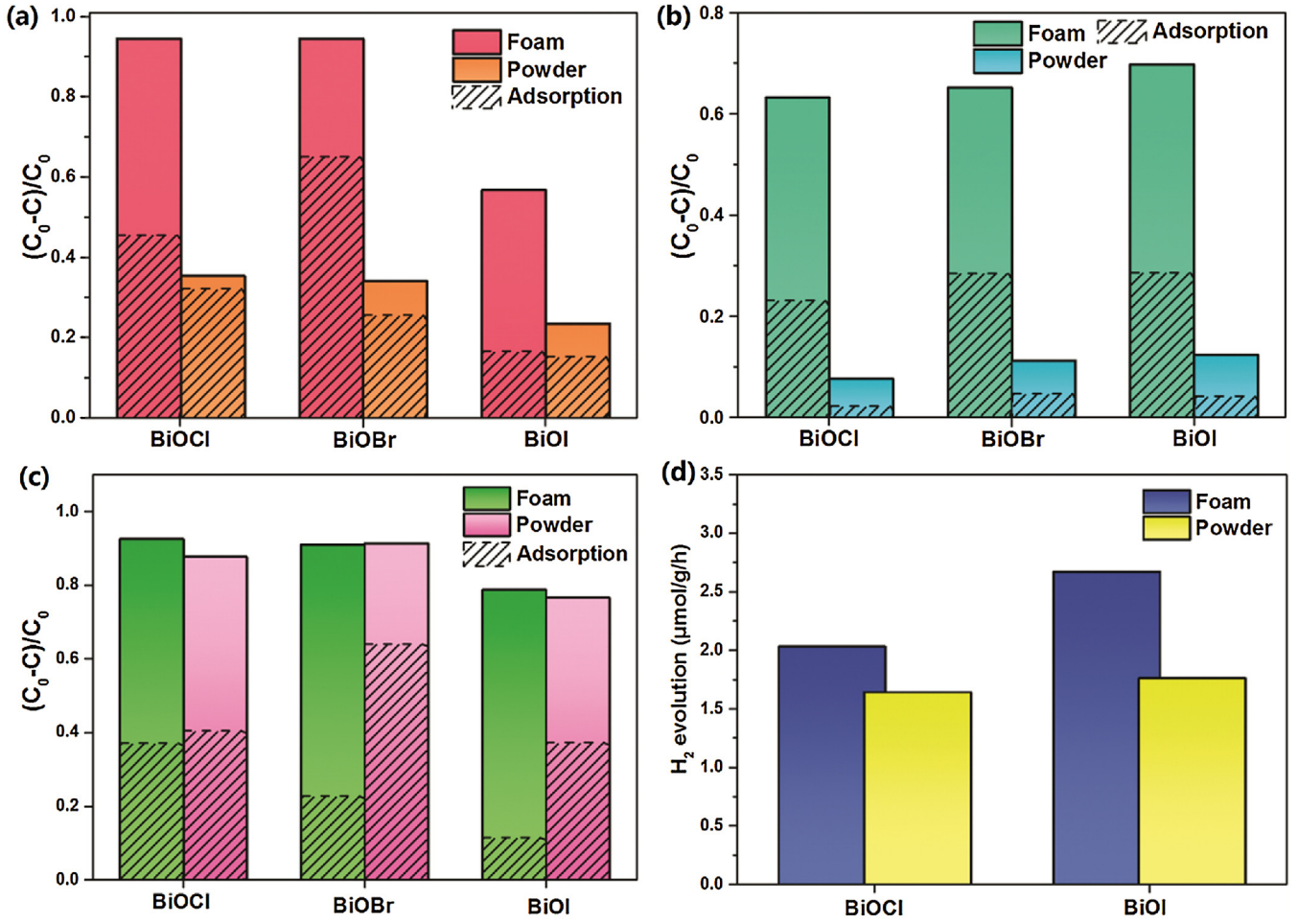

Fig. 4. Adsorption in darkness and photocatalytic degradation of (a) MO, (b) phenol and (c) chlortetracycline and (d) photocatalytic H_2 evolution rate under simulated solar light.

der and PUF based-BiOX photocatalyst, the same equivalent weight of BiOX was strictly controlled. First, azo dye model methyl orange (MO) was chosen as the target, which is a negatively charged dye and can be adsorbed on the surface of BiOX. Thus, it can indicate both the adsorption and photocatalysis effects. The adsorption and degradation degree of contaminants in water was examined by

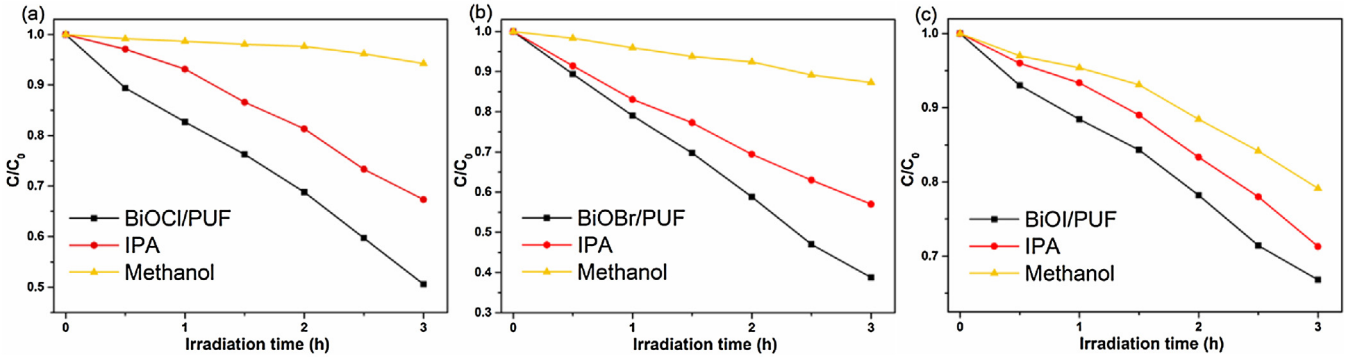

Fig. 5. Photocatalytic degradation of MO over (a) BiOCl/PUF, (b) BiOBr/PUF and (c) BiOI/PUF photocatalysts alone and with the addition of IPA, or Methanol.

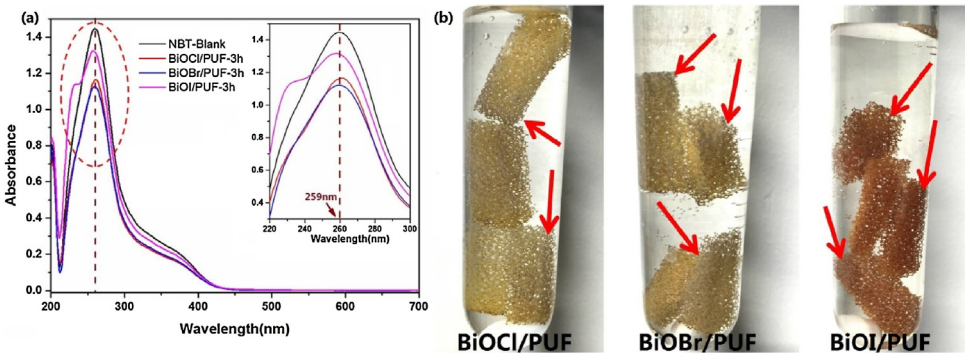

Fig. 6. (a) Absorption spectra of NBT over BiOX/PUF and (b) pictures after NBT transformation demonstrating the blue diformazan adsorbing on the surface of BiOX/PUF. (For interpretation of the references to colour in this figure legend, the reader is referred to the web version of this article.)

determining the change in their characteristic absorption peaks (Fig. S6). The BiOX powders show poor degradation activity in contrast to the relatively strong adsorption (Fig. 4a). When BiOX and PUF were combined to construct PUF based-BiOX foam photocatalysts, it was seen that both the adsorption and photocatalytic abilities of BiOX/PUF are largely improved compared with the powder counterparts, e.g. for BiOBr, the adsorption and photocatalytic abilities increase 2.5 and 2.8 folds, respectively. The characteristic absorption peak of MO in 464 nm gradually decreases with prolonging irradiation time (Fig. S6), revealing the gradual decomposition of MO. Phenol, a typical industrial contaminant that can lead to tissue necrosis of body and animals, was employed here to further indicate the photocatalytic activity. It is amazing to observe that BiOX/PUF has a super performance in treating phenol. The adsorption and photodegradation efficiencies of phenol over BiOX/PUF significantly strengthened, which are approximately 10 and 8 times higher than these powders, respectively (Fig. 4b). In order to exclude the adsorption capability of PUF, the adsorption of phenol over bare PUF was monitored. The limited adsorption ratio of PUF can be ignored in contrast to the dramatically enhanced activity of BiOX/PUF (Fig. S7). The time-resolved absorbance spectra confirmed that phenol molecules are destroyed by BiOX/PUF (Fig. S8). Chlortetracycline is used extensively for growth promotion and therapeutic purposes in livestock production. whereas, the overuse of chlortetracycline in agriculture also causes environmental pollution. Herein, it was also employed to further confirm the unselective photocatalytic activity of BiOX/PUF. Though BiOX powder shows much stronger adsorption property, BiOX/PUF presents better photocatalytic activity, in which the degradation efficiency increases 1.2–2.5 folds compared with the powder counterpart (Fig. 4c). Over all, BiOX/PUF foams reveal powerful ability in treating various contaminants in contrast to BiOX powder.

These results are understandable, because the spongy PUF can act as an excellent substrate to prevent aggregation of the BiOX nanosheets and render its even dispersion on PUF. It is postulated that the BiOX/PUF foams show a much larger specific surface area compared with the BiOX powder, and thus, BiOX/PUF foams display higher adsorption capability toward MO than the BiOX powder. As shown in Fig. 4a, 63% of MO can be adsorbed over the BiOBr/PUF whereas only 23% over the pure BiOBr powder. Generally, the photocatalyst with a good adsorption capability is a vital prerequisite for high photocatalytic degradation. In addition, the array-like arrangement of BiOX nanosheets enables them to dominantly expose their {001} facets, which are the active facets of BiOX, as evidenced by the SEM and HRTEM images (Fig. 2c and e). The strong internal electric field derived from highly exposed {001} active facets, which benefits charge separation and transportation, leading to a more efficient photocatalytic degradation. It was strongly evidenced by the above chlortetracycline degradation result (Fig. 4c). BiOX/PUF foams show much lower absorbability in chlortetracycline in contrast to the powdery BiOX, whereas the foams demonstrate profoundly strengthened photodegradation performance.

Moreover, photocatalytic water splitting H_2 production from water over BiOX/PUF foams was also monitored. The H_2 production rates of BiOCl/PUF and BiOI/PUF in methanol aqueous solution are shown in Fig. 4d. Herein, no H_2 production was detected over BiOBr powder or BiOBr/PUF, which may be due to the inappropriate band energy level of BiOBr for H_2 evolution. From Fig. 4d, it is obvious BiOCl/PUF and BiOI/PUF also show enhanced H_2 evolution rates than the powder counterparts, with improvement of 23.8% and 51.7%, respectively. This result discloses these spongy foam photocatalysts may also have potentials in renewable energy field.

To reveal the photocatalytic mechanism of BiOX/PUF photocatalysts, the active species trapping experiments were used to

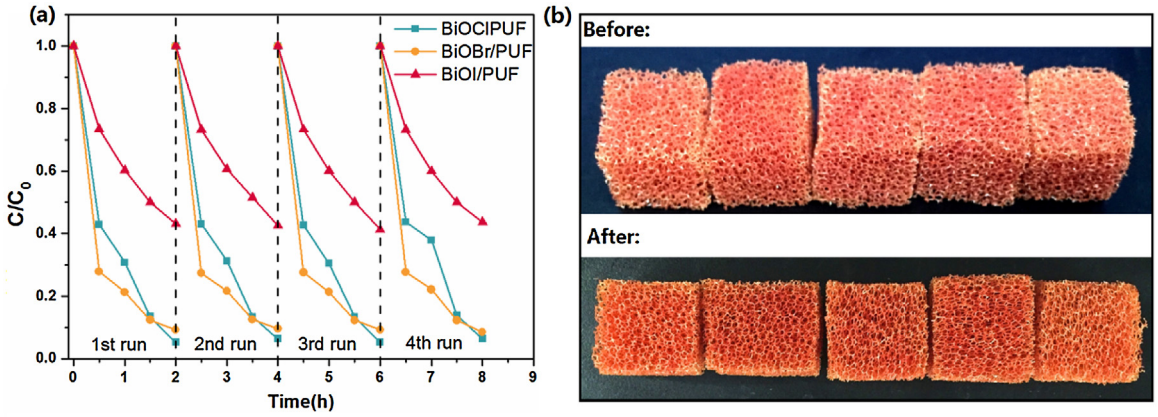

Fig. 7. (a) Cycling runs under simluated solar light. (b) BiOI/PUF foam photocatalysts before and after 4 recycling degradation process.

determine the main radicals in the photocatalytic process. For BiOCl/PUF, the degradation efficiency of MO is decreased slightly upon addition of IPA, suggesting that hydroxyl radicals •OH are not the main active species for the MO photodegradation (Fig. 5a) [36]. However, when the methanol was added for holes h^+, the degradation of MO is significantly decreased. In addition, NBT as a scavenger of $^{\bullet}O_2^-$ also has been consumed significantly as in Fig. 6a. Due to the super adsorption capability of BiOX/PUF, the blue diformazan (a reaction product of NBT with $^{\bullet}O_2^-$) is adsorbed on the surface of BiOCl/PUF, and part of the BiOCl/PUF surface turned to blue or purple (Fig. 6b). Thus, the results showed that $^{\bullet}O_2^-$ and h^+ are the main reactive species of BiOCl/PUF, while ·OH plays little role in the degradation of MO. For BiOBr/PUF, •OH are also not the main active species for the MO photodegradation (Fig. 5a). But, when the methanol was added for trapping holes (h^+), the degradation of MO is significantly decreased. With the decreasing of NBT, part of the BiOBr/PUF surface also turned to blue or purple (Fig. 6b). Similarly, the results of BiOBr/PUF also showed that $^{\bullet}O_2^-$ and h^+ are the main reactive species, while •OH plays little role in the degradation of MO. For BiOI/PUF, ·OH and h^+ are not the main active species for the MO photodegradation (Fig. 5c), and NBT result shows that only $^{\bullet}O_2^-$ is the main reactive specie in the degradation process (Fig. 6).

In addition to the strong photo-degradation and H_2 evolution capability, other properties, such as high stability, easy recovery, good reusability and recyclability, are indispensable in practical photocatalysis application. First, the stability of BiOX/PUF is studied. It can be seen that almost 98% of the original photocatalytic activity can be maintained after four cycles (Fig. 7a). There is also no change occurred on the appearance of BiOX/PUF (like collapse of BiOX/PUF framework, separation of BiOX nanosheets from PUF, etc) in continuous photodegradation reaction for 8 h (Fig. 7b). For BiOX powder, almost only 50% of the original photocatalytic activity can be maintained just after three cycles (Fig. S9a and b). The above experiments demonstrated the high stability and durability of BiOX/PUF. Secondly, the BiOX/PUF can be easily separated and recycled from the solutions by a tweezer without loss of any solid photocatalysts after the aqueous photocatalytic reaction, which assures the excellent recovery performance (Fig. 8a). On the contrary, although the BiOX powder is also stable during the photocatalytic reaction, the recycling process via filtration leads to inevitable loss of photocatalyst. In addition, BiOX/PUF is spongy and flexible (Fig. 8a), enabling it to be suitable for any photo-degradation or hydrogen production reactor, which broadens the application scope. Moreover, the density of BiOX/PUF is tunable by controlling the dipping cycle times in the synthesis process (Scheme 1 and Fig. 8b). BiOX/PUF can not only float on the water, but also be suspended in the water as well as sink in

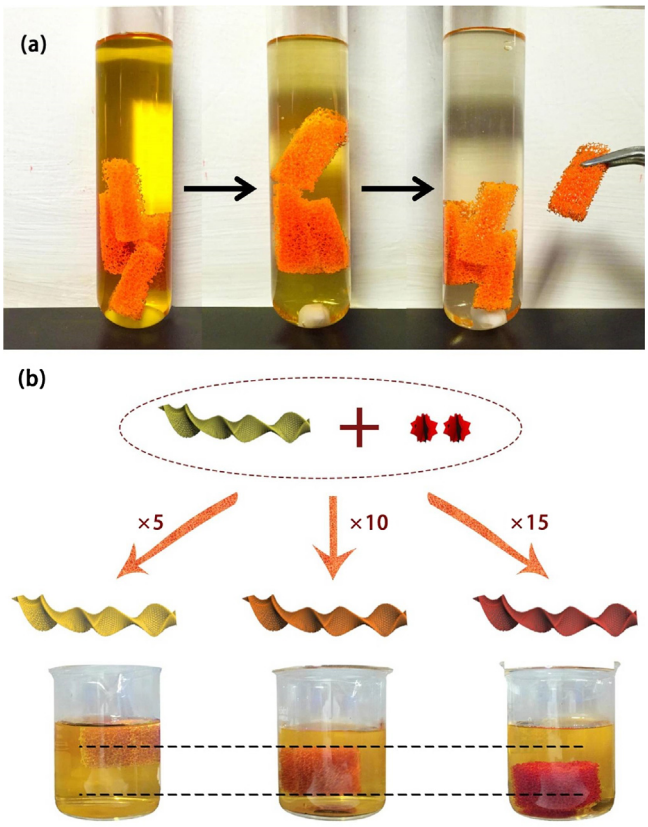

Fig. 8. (a) Recycling of flexible BiOI/PUF using a tweezer and (b) controllable density of BiOI/PUF.

the bottom of the water. To optimize the loading ratio of BiOX on PUF, six kinds of BiOI/PUF with different loading amounts were tested by MO (50 mL, 2×10^{-5} mol/L) photodegradation evaluation. As shown in Fig. 9a and b, the sample with dipping times of 25 shows the highest degradation activity and the 15 dipping times sample shows the lowest activity. The mass of BiOI in BiOI/PUF with dipping times of 25 is 107 mg. In addition, we also test the photodegradation activity of BiOX/PUF foam with different sizes. It is demonstrated that there is negligible change in photodegradation efficiency between the foams with sizes of $2 \times 2 \times 1.5\ cm^3$ and $1 \times 1 \times 1.5\ cm^3$ (Fig. S10). These results show that BiOX/PUF could balance the utilization of solar energy and adequate contact with contaminants, better adapting to the practical wastewater purification in the river. Therefore, in addition to its superior photocatalytic

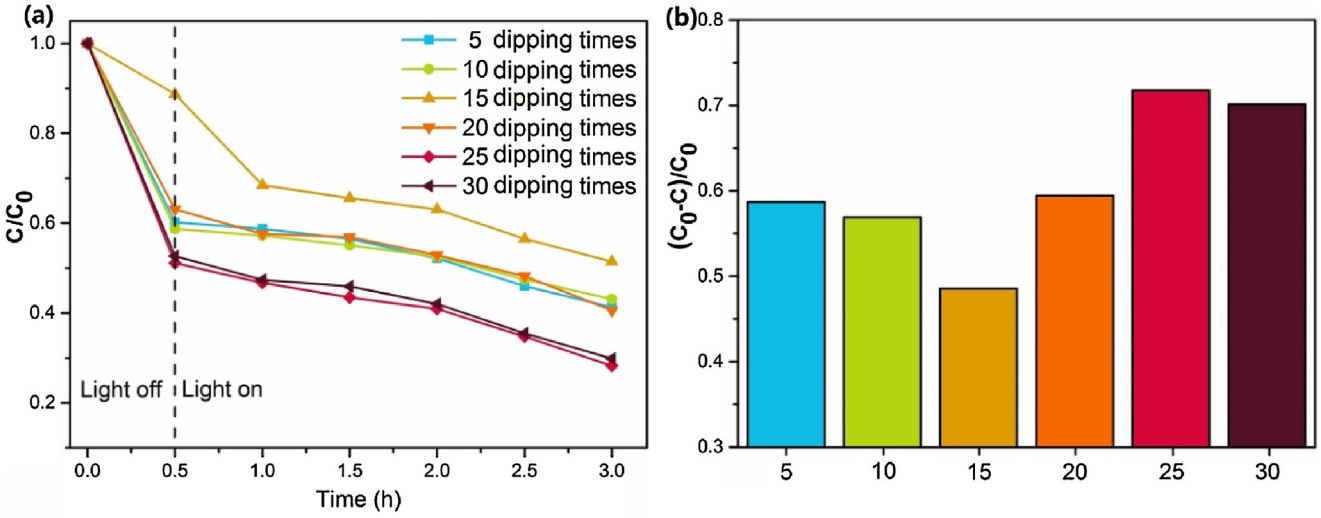

Fig. 9. (a) Photocatalytic MO degradation curves of six kinds of BiOI/PUF with different loading amounts and (b) the corresponding degradation efficiencies.

performance, the BiOX/PUF also shows multiform attractive merits in stability, recovery, recycling, controllability and adaptability, which are especially important for the practical applications.

4. Conclusions

In summary, BiOX/PUF spongy foam photocatalytsts were obtained via a facile dipping-hydrolysis process. PUF as an excellent substrate is very stable and shows a strong electric attraction for BiOI powder. And therefore it enables BiOX to evenly distribute on the PUF surface with a nanosheet-array-like arrangement and renders enhanced surface area and high exposure of BiOX {001} active facets. The strong internal electric field derived from high exposed {001} active facets benefits charge separation and transportation. The BiOX/PUF foams thus present not only significantly promoted photocatalytic activity for degradation of azo dye, phenol and antibiotic, but also enhanced photocatalytic H_2 evolution. Moreover and significantly, BiOX/PUF foams show high stability, easy recovery, good recycling and excellent controllability and adaptability, strongly boding for its promising practical prospect. The photocatalysis mechanism of BiOX/PUF foam photocatalysts has also been revealed. The dipping-hydrolysis method is expected to be a general strategy for preparation of other foam photocatalysts. Our work may open up a new avenue for developing high-performance photocatalytic materials for practically environmental remediation and renewable energy generation.

Acknowledgements

This work was jointly supported by the National Natural Science Foundations of China (Grant No. 51672258, 51302251 and 51572246), the Fundamental Research Funds for the Central Universities (2652015296).

Appendix A. Supplementary data

Supplementary data associated with this article can be found, in the online version, at http://dx.doi.org/10.1016/j.apcatb.2017.02.033.

References

[1] L.B. Kreuzer, C.K.N. Patel, Science 173 (1971) 45–47.
[2] F.M. Anne, M.T. Dulay, Chem. Rev. 93 (1993) 341–357.
[3] M.A. Shannon, P.W. Bohn, M. Elimelech, J.G. Georgiadis, B.J. Mariñas, A.M. Mayes, Nature 452 (2008) 301–310.
[4] M. Elimelech, W. Phillip, Science 333 (2011) 712–717.
[5] M. Chong, B. Jin, C.W.K. Chow, C. Saint, Water Res. 44 (2010) 2997–3027.
[6] N. Tian, Y. Zhang, H. Huang, Y. He, Y. Guo, J. Phys. Chem. C. 118 (2014) 15640–15648.
[7] S.N. Frank, J.B. Allen, J. Phys. Chem. C 81 (1977) 1484–1488.
[8] R.W. Matthews, Water Res. 25 (1991) 1169–1176.
[9] M.J. Sampaio, R.R. Bacsa, A. Benyounes, R. Axet, P. Serp, C.G. Silva, A.M.T. Silva, J.L. Faria, J. Catal. 331 (2015) 172–180.
[10] H. Li, S. Yin, Y. Wang, T. Sekino, S.W. Lee, T. Sato, J. Catal. 297 (2013) 65–69.
[11] Y. Myung, F. Wu, S. Banerjee, A. Stoica, H. Zhong, S. Lee, J. Fortner, L. Yang, P. Banerjee, Chem. Mater. 27 (2015) 7710–7718.
[12] K. Zhao, L. Zhang, J. Wang, Q. Li, W. He, J. Yin, J. Am. Chem. Soc. 135 (2013) 15750–15753.
[13] B. Zhang, J. Li, B. Zhang, R. Chong, R. Li, B. Yuan, S. Lu, C. Li, J. Catal. 332 (2015) 95–100.
[14] F. Teng, Z. Liu, A. Zhang, M. Li, Environ. Sci. Technol. 49 (2015) 9489–9494.
[15] L. Kong, M. He, Environ. Sci. Technol. 50 (2016) 6974–6982.
[16] N. Zhang, M. Yang, Z. Tang, Y. Xu, J. Catal. 303 (2013) 60–69.
[17] C. Zeng, Y. Hu, Y. Guo, T. Zhang, F. Dong, Y. Zhang, H. Huang, ACS Sustain. Chem. Eng. 4 (2016) 3305–3315.
[18] H. Huang, X. Han, X. Li, S. Wang, P.K. Chu, Y. Zhang, ACS Appl. Mater. Interfaces 7 (2015) 482–492.
[19] S. Yu, H. Huang, F. Dong, M. Li, N. Tian, T. Zhang, Y. Zhang, ACS Appl. Mater. Interfaces 7 (2015) 27925–27933.
[20] H. Shi, J. Chen, G. Li, X. Nie, H. Zhao, P. Wong, T. An, ACS Appl. Mater. Interfaces 5 (2013) 6959–6967.
[21] H. Yin, X. Chen, R. Hou, H. Zhu, S. Li, Y. Huo, H. Li, ACS Appl. Mater. Interfaces 7 (2015) 20076–20082.
[22] Y. Guo, Z. Ren, W. Xiao, C. Liu, H. Sharma, H. Gao, A. Mhadeshwar, P. Gao, Nano Energy 2 (2013) 873–881.
[23] K. Oppelt, J. Gasiorowski, D. Egbe, J. Kollender, M. Himmelsbach, A. Hassel, N. Sariciftci, G. Knör, J. Am. Chem. Soc. 136 (2014) 12721–12729.
[24] L. Wang, J. Ge, A. Wang, M. Deng, X. Wang, S. Bai, R. Li, J. Jiang, Q. Zhang, Y. Luo, Y. Xiong, Angew. Chem. Int. Ed. 53 (2014) 5107–5111.
[25] S. Bai, X. Li, Q. Kong, R. Long, C. Wang, J. Jiang, Y. Xiong, Adv. Mater. 27 (2015) 3444–3452.
[26] T. Kim, K. Choi, Science 343 (2014) 6174–6179.
[27] H. Li, J. Shang, Z. Ai, L. Zhang, J. Am. Chem. Soc. 137 (2015) 6393–6399.
[28] M. Guan, C. Xiao, J. Zhang, S. Fan, R. An, Q. Cheng, J. Xie, M. Zhou, B. Ye, Y. Xie, J. Am. Chem. Soc. 135 (2013) 10411–10417.
[29] J. Jiang, K. Zhao, X. Xiao, L. Zhang, J. Am. Chem. Soc. 134 (2012) 4473–4476.
[30] H. Engels, H. Pirkl, R. Albers, R. Albach, J. Krause, A. Hoffmann, H. Casselmann, J. Dormish, Angew. Chem. Int. Ed. 52 (2013) 9422–9441.
[31] Y. Kim, J. Zhu, B. Yeom, M.D. Prima, X. Su, J. Kim, S.J. Yoo, C. Uher, N.A. Kotov, Nature 500 (2013) 59–63.
[32] H.O. Ham, Z. Qu, C.A. Haller, B.M. Dorr, E. Dai, W. Kim, D.R. Liu, E.L. Chaikof, Nat. Commun. 7 (2015) 11140–11148.
[33] M.G. Kibria, F.A. Chowdhury, S. Zhao, B. Alotaibi, M.L. Trudeau, H. Guo, Z. Mi, Nat. Commun. 6 (2015) 6797–6805.
[34] X. Huang, C. Tan, Z. Yin, H. Zhang, Adv. Mater 26 (2014) 2185–2204.
[35] X.W. Wang, G. Liu, Z.G. Chen, F. Li, L.Z. Wang, G.Q. Lu, H.M. Cheng, Chem. Commun. (2009) 3452–3454.
[36] N. Tian, H. Huang, C. Liu, F. Dong, T. Zhang, X. Du, S. Yu, Y. Zhang, J. Mater. Chem. A 3 (2015) 17120–17129.